EXPERIMENTAL DETERMINATION OF TURNING ANGLE AND LOSSES OF AXIAL COMPRESSOR INLET GUIDE VANES

William Richard Wheeler

NAVAL POSTGRADUATE SCHOOL
Monterey, California

THESIS

EXPERIMENTAL DETERMINATION OF
TURNING ANGLE AND LOSSES OF AXIAL
COMPRESSOR INLET GUIDE VANES

by

William Richard Wheeler

Thesis Advisors: M.H. Vavra
P.F. Pucci

December 1972

Approved for public release; distribution unlimited.

Experimental Determination of Turning Angle and Losses of Axial Compressor Inlet Guide Vanes

by

William Richard Wheeler
Lieutenant, United States Navy
B.S.E., University of Michigan, 1966

Submitted in partial fulfillment of the
requirements for the degree of

MASTER OF SCIENCE IN MECHANICAL ENGINEERING

from the

NAVAL POSTGRADUATE SCHOOL
December 1972

ABSTRACT

This investigation experimentally determined the minimum loss incidence angle, deviation angle, and total-pressure loss coefficient for a cascade with airfoil-type blade profiles used as inlet guide vanes for an axial-flow compressor with an equivalent camber angle of 37.6 degrees and unit solidity. The experimental values were compared with values predicted using correlations based on compressor cascade tests.

TABLE OF CONTENTS

TABLE OF NOTATION

D	Diffusion Factor
H	Wake Form Coefficient
K	Correction Factors
P_t	Total Pressure
P_k	Kiel Probe Total Pressure
P	Static Pressure
Q	Dynamic Pressure
V	Velocity
Y	Total-Pressure Loss Coefficient
Z	Axial Direction
c	Chord Length
i	Incidence Angle
s	Blade Spacing
t	Blade Thickness
β	Air Angle
γ	Blade-Chord Angle
δ	Deviation Angle
θ^*	Wake Momentum Thickness
λ	Total-Pressure Function
ν	Dynamic Pressure Function
σ	Solidity
ϕ	Blade-Camber Angle

SUBSCRIPTS

0	Zero-Camber Angle
1	Inlet Measuring Plane
2	Outlet Measuring Plane
10	For Ten Percent Blade Thickness NACA 65 blade
ref	Reference
loc	Local
sh	Shape

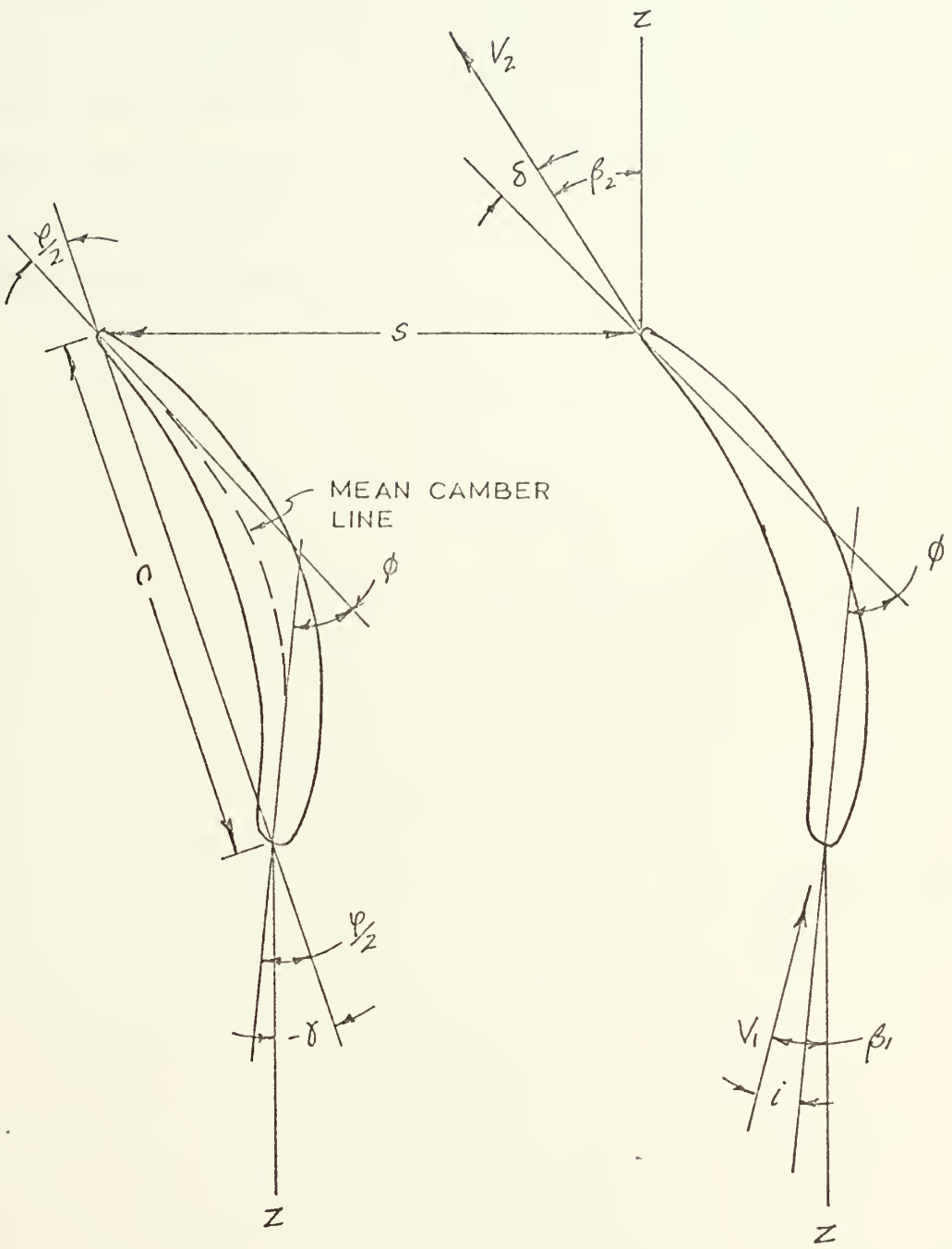

FIGURE 1. Blade angle nomenclature.

ACKNOWLEDGEMENT

The author gratefully acknowledges the guidance and advice given by Professor M. H. Vavra of the Department of Aeronautics and Professor P. F. Pucci of the Department of Mechanical Engineering and the willing cooperation and competent assistance provided by Mr. R. W. Savage of the Turbopropulsion Laboratory.

I. INTRODUCTION

Most axial-flow compressors, particularly those operating with a degree of reaction of 50%, require inlet guide vanes that produce the necessary whirl components of the flow ahead of the first rotor blade. Since flow deflection in these inlet guide vanes (IGV, for short) is considerably smaller than the flow deflections in turbine bladings, the design principles of the latter cannot be applied with sufficient accuracy. On the other hand the flow in the IGV is accelerated - in contrast to that in an axial flow rotor, where it is decelerated. It is however, possible for IGV to use airfoil-shaped profiles of the same type as in rotor bladings.

Presently there are no design correlations available which enable the designer to predict the so-called deviation angle of the flow. The deviation angle is the angle between the direction of the flow leaving the trailing edge of the blade and the tangent to the mean camber line at the trailing edge of the blade.

The designer is also unable to predict the total-pressure loss coefficient defined as the ratio of the loss of total pressure in the IGV to the inlet dynamic pressure.

The objectives of this investigation were to compare the characteristics of the IGV, which can be determined with the correlations of Chapter VI of Ref. 1 by assuming

them to operate as compressor blades, with tests conducted in the Rectilinear Cascade Facility of the Turbopropulsion Laboratory at the Naval Postgraduate School.

II. NATURE OF INVESTIGATION

A. PURPOSE OF INVESTIGATION

The redesign of the low-speed axial-flow compressor test rig at the Turbopropulsion Laboratory, Naval Postgraduate School, for investigations of tip clearance effects, pointed out the lack of design information on IGV. Information was desired to determine the deviation angle for the minimum loss conditions of the IGV for unit solidity and the C-4 blade profile which were to be used.

B. AREA OF INVESTIGATION

Extensive testing resulting in large amounts of data has been conducted on both compressor and turbine cascades. This data has been analyzed and correlations have been determined for the design of efficient compressor and turbine blades.

The IGV are similar to compressor blades in that they are normally used in the same range of solidity, have the same range of turning angles, and have similar shape. On the other hand, IGV are like turbine blades, accelerating the flow in them. Because of these conditions, neither turbine nor compressor correlations can be applied to the design of IGV with sufficient accuracy.

The objective of this investigation was to conduct a series of cascade tests on a standard blade section as used for IGV. The results of the tests would be compared to

values of deviation angle and loss coefficient calculated using correlations based on compressor cascade data. A NACA 65 series blade section was used for the tests because these blades were available in the laboratory and the results could be applied to the C-4 circular arc blades to be used as IGV in the test compressor.

C. CORRELATIONS

Some correlations of the data from previous cascade testing of compressor blades are given in Chapter VI of Ref. 1. The correlations were established for NACA 65 series blades with a thickness ratio of ten percent. Correction factors are applied to certain parameters in the calculations for other blade thicknesses and thickness distributions. These values are given in Ref. 1 for the C-4 series blades. Because the Mach number was less than 0.25, corrections for Mach number could be neglected.

The correlations were derived using a reference location at the minimum point on the total-pressure loss coefficient versus incidence angle curve. For compressor cascades at low Mach number, this region of the curve is generally flat and the reference point is taken as the midpoint of the region.

1. Reference Incidence Angle

The determination of the reference incidence angle is done in two steps. The first is the determination of the reference, minimum loss incidence angle for the blade with

zero camber. The second step is the correction of this value for blade camber.

The zero-camber incidence angle is expressed as

$$i_0 = (K_i)_{sh} (K_i)_t (i_0)_{10} \qquad (1)$$

where $(i_0)_{10}$ is the zero-camber incidence angle for the ten-percent thick 65 series blades. $(K_i)_{sh}$ and $(K_i)_t$ are thickness and shape correction factors for blades other than the NACA 65-series. The value of $(i_0)_{10}$ is obtained from Fig. 137 of Ref. 1 as function of solidity and inlet-air angle. $(K_i)_{sh}$ and $(K_i)_t$ are unity for the blades under study.

The correction for camber takes the form of

$$i_{ref} = i_0 + n\phi \qquad (2)$$

where ϕ is the camber angle of the blade and n is the slope of the incidence-angle variation with camber curve found in Fig. 138 of Ref. 1, again as function of solidity and inlet-air angle.

2. Deviation Angle

The reference deviation angle can be found by the deduced method, or by Carter's Rule.

The deduced method is similar to the reference incidence angle determination. A zero-camber deviation angle is obtained from Fig. 161 Ref. 1, for given solidity and inlet-air angle. This value is corrected for blade thickness and thickness distribution as in equation 1. The

reference deviation angle is then determined from

$$\delta_{ref} = \delta_o + m\phi \tag{3}$$

where δ_o is the zero-camber deviation angle and m is the slope of the deviation-angle variation with camber curve, obtained from Fig. 162 Ref. 1 as a function of solidity and inlet-air angle.

Carter's rule is given as

$$\delta_{ref} = \frac{m_c \phi}{\sigma} \tag{4}$$

where m_c is a function of blade-chord angle, given by Fig. 2, which is an extrapolation of Fig. 160 Ref. 1 for the region of negative blade-chord angles. This line can be used for both NACA 65 and C-4 series blades.

The deviation angle, using either of the δ_{ref} values, is expressed as

$$\delta = \delta_{ref} + (i - i_{ref}) \left(\frac{d\delta}{di}\right)_{ref} \tag{5}$$

where $\left(\frac{d\delta}{di}\right)_{ref}$ represents the slope of the deviation angle variation at the reference incidence angle. This value is obtained from Fig. 177 Ref. 1 as a function of inlet-air angle and solidity.

3. Loss Coefficient

The total-pressure loss coefficient was used to compare the losses across the IGV. This coefficient is defined as

$$Y = \frac{P_{t1} - P_{t2}}{Q_1} \tag{6}$$

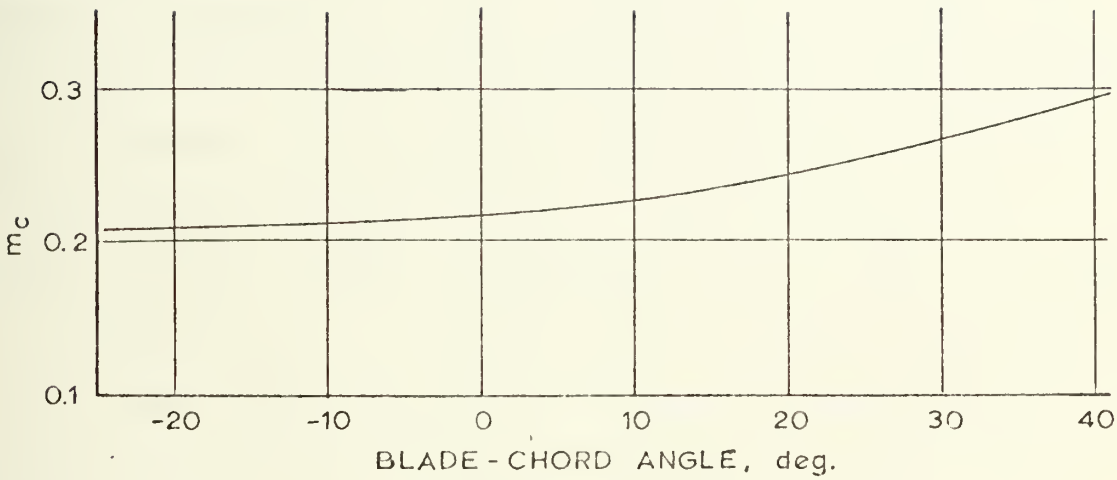

FIGURE 2. Extrapolation of Fig. 160 Ref. 1 for values of the Carter's rule parameter m_c for circular arc blades, to negative values of blade-chord angle.

The determination of the coefficient by either of the two methods of Chapter VI Ref. 1 is based on the local diffusion factor

$$D_{loc} = \frac{V_{max} - V_2}{V_{max}} \tag{7}$$

where V_{max} is the maximum suction-surface velocity. This factor is a measure for the decceleration of the flow over the blade surface which is directly related to the boundary layer formation. The boundary layer causes the formation of the wake and a major portion of the resulting losses. However, in the cascade configuration under study, the flow is accelerated with a resulting positive pressure gradient in the blade channel and not a deceleration with adverse pressure gradient as occuring in compressor blades. The formation of the boundary layer is different due to the different pressure gradients and the diffusion factor is in effect undefined and not applicable.

However for the purpose of this investigation, the diffusion factor is assumed to be valid and it will be used to determine the loss coefficients. Because a continuous measurement of velocity along the blade surface is not practical, the diffusion factor has been redefined as[1]

$$D = (1 - \frac{V_2}{V_1}) + \frac{\Delta V}{2\sigma V_1} \tag{8}$$

---

[1]This can be done for compressor blades because the pressure (velocity) distribution on the blade is of the shape shown in Fig. 13(10) of Ref. 2 and equation 8 will approximate equation 7.

where the velocities are shown in Fig. 147 of Ref. 1. The velocity diagram for an inlet guide vane is shown in the Figure below.

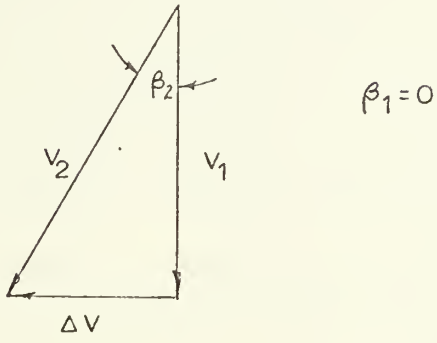

These conditions lead to the equation

$$D = 1 - \cos \beta_2 + \frac{\tan \beta_2}{2\sigma} \qquad (9)$$

Actually, two methods could be used to find Y. With the first the diffusion factor is used as an input to Fig. 149(b) Ref.1 to obtain a value of $\frac{Y \cos \beta_2}{2\sigma}$ from which Y can be calculated. For reference this method is called method 1.

The other method consists in using the diffusion factor in Fig. 148 Ref. 1 to determine a value for the momentum-thickness ratio. This value and an estimate for the wake form factor H_2 are substituted into equation 264 of Ref. 1 to determine Y. This approach is called method two.

Again it should be emphasized that these correlations were derived for compressor cascades where the flow is decelerated.

D. REQUIREMENTS FOR THE TEST FACILITY

Initial calculations of the total-pressure loss coefficient indicated that a value in the range of 0.01 could be expected. To this value would correspond an average total pressure drop across the blades of about 0.25 inches of water and would even be smaller outside of the blade wake. To ensure accurate measurement, a steady state situation and uniform inlet conditions were needed in the cascade. Also required to model IGV conditions was an inlet-air angle of zero.

1. Steady State Approximation

The cascade test rig used to conduct the test was affected by power and atmospheric variations. This caused fluctuations of the flow conditions in the cascade, resulting in a variation of inlet total pressure of as much as 0.20 inches of water over a 15 minute period. This was considered too great a variation for accurate results.

The use of a reference pressure in the flow ahead of the cascade which varied in the same manner as the other pressures was used as a solution. No modifications were possible to the cascade facility in the time available to reduce the fluctuations. The reference pressure used was the total pressure sensed by a Kiel probe at a fixed location upstream of the inlet measuring plane.

The pressure data taken in the cascade was then reduced into a flow function dependent on value measured

and reference pressure. The two functions used in the tests were

$$\lambda = \frac{P_t - P_{atm}}{P_k - P_{atm}} \qquad \nu = \frac{Q}{P_k - P_{atm}} \tag{10}$$

where P_k is the Kiel probe total pressure. For data reduction an average Kiel probe total-pressure value was used as a reference.

2. Inlet Conditions

Work was done by Bartocci in 1964 [Ref.3] to improve the inlet conditions of the cascade test facility. However a survey of the inlet of the test section showed variations of over ten percent in total pressure with inlet vanes. Without inlet vanes the pressure was more uniform, however, the inlet-air angle varied up to five degrees across the measuring plane. Wire screen placed across the inlet did not improve the conditions, but merely reduced the flow velocity through the test section.

The conditions at the center of the inlet measuring plane, ahead of the center blade, without inlet vanes and wire screen were uniform in total pressure to one percent and constant in inlet-air angle to within ±.75 degrees. The tests were carried out at this location to obtain the most accurate results.

III. METHOD OF INVESTIGATION

The tests of the inlet guide vanes were conducted in the Rectilinear Cascade Test Facility of the Turbopropulsion Laboratory at the Naval Postgraduate School, Monterey, California. A schematic of the general arrangements of the test facility is shown in Fig. 3. The cascade is an open cycle wind tunnel in which a number of identical axial-flow turbomachine blades arranged along a straight axis can be tested. The rectilinear cascade is an approximation of the blading arrangment in axial-flow turbomachines; however, if enough blades are used the periodicity of the exit flow duplicates the exit flow in actual machinery closely enough to give valid results.

A detailed description of the test facility as installed was given by Rose and Guttormson [Ref. 4]. Modifications and changes to the facility have been made to improve the flow in the test section and to increase the accuracy of the instrumentation. These changes were described by Bartocci [Ref. 3 and 5] and Woods [Ref. 6].

A. EXPERIMENTAL ARRANGEMENTS

The cascade arrangement for the tests was as shown in Figs. 4 and 5. The cascade consisted of seven blades with a spacing of eight inches. The side walls were parallel with an angle of two degrees from vertical to produce axial flow ahead of the blades.

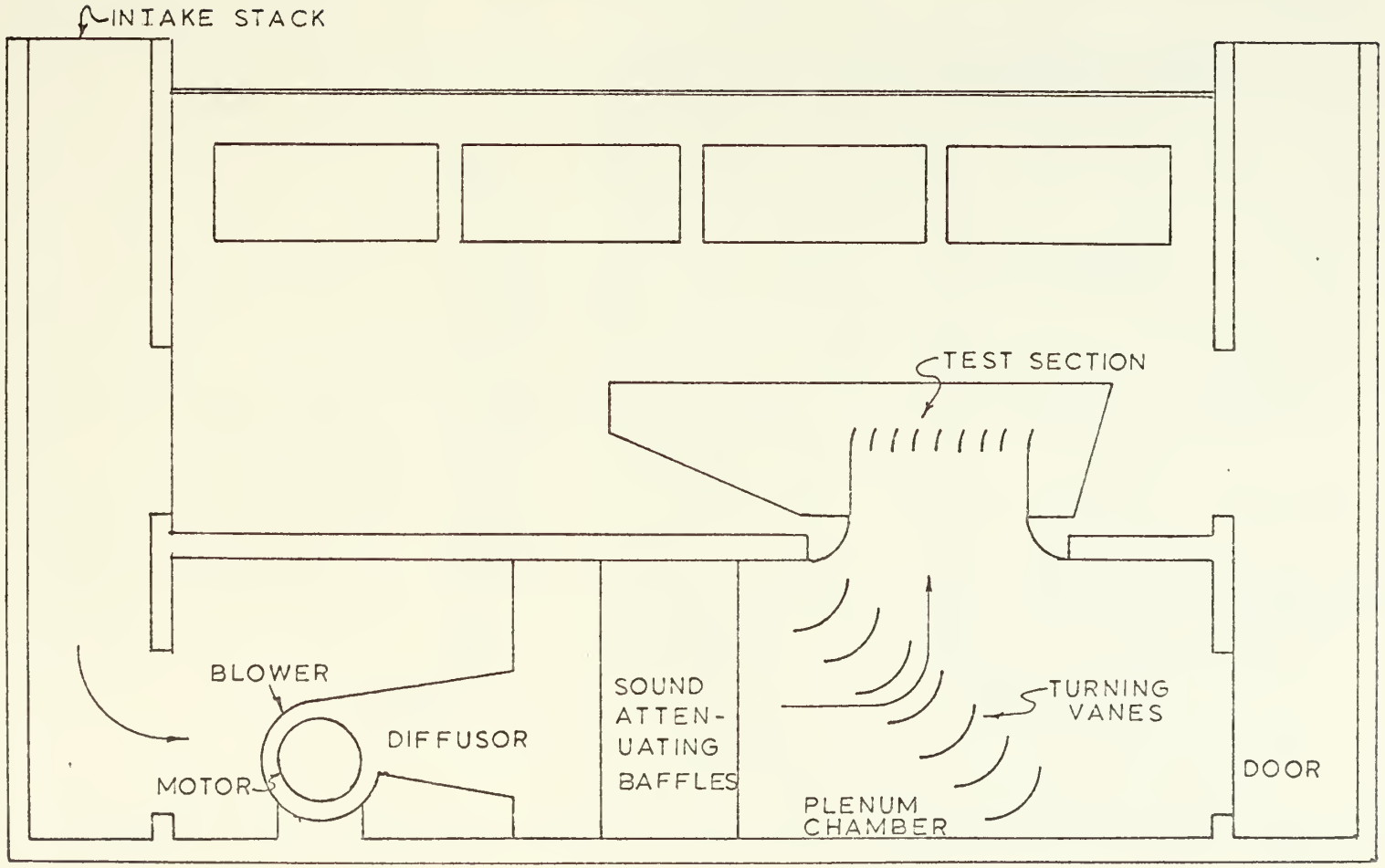

FIGURE 3. Rectilinear Cascade Test Facility general arrangement.

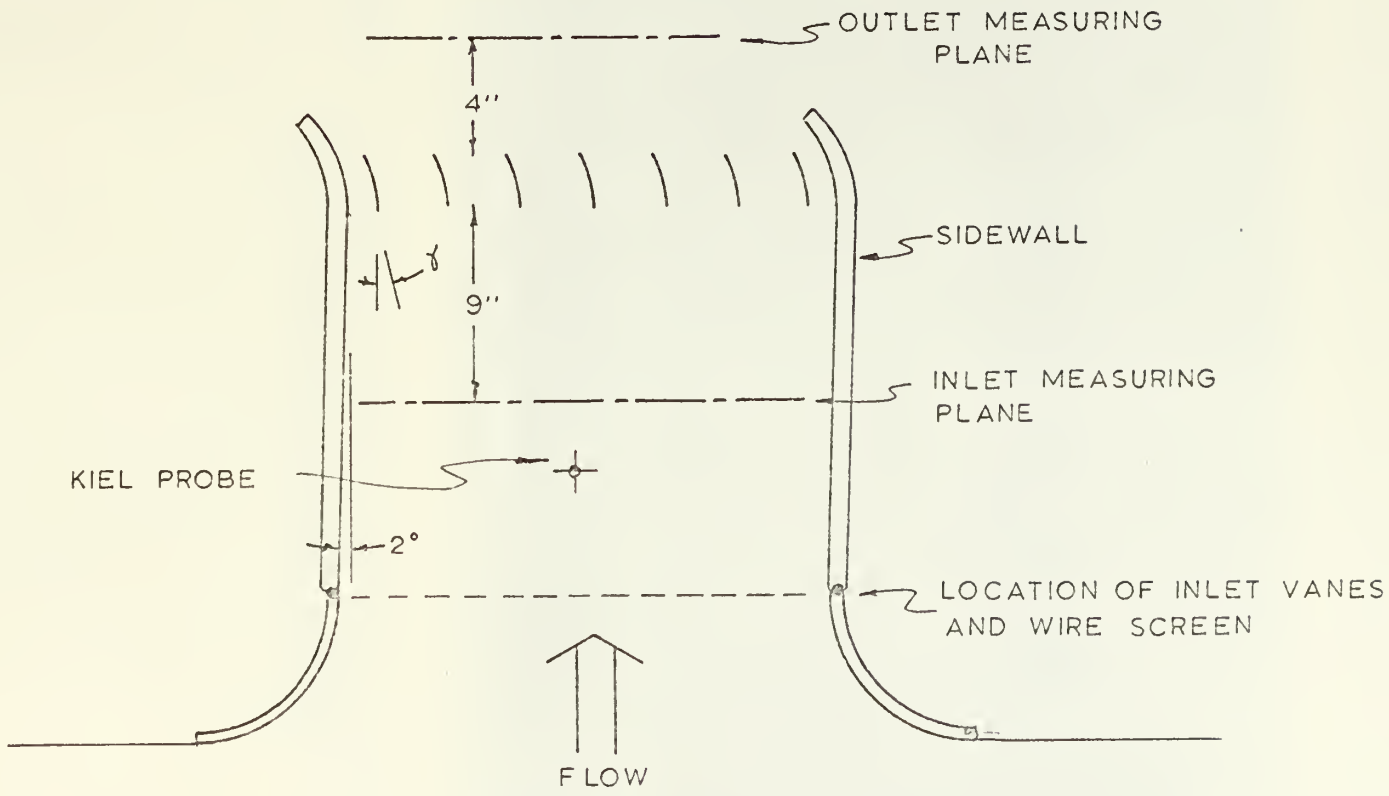

FIGURE 4. Arrangement of cascade test section for tests of inlet guide vanes.

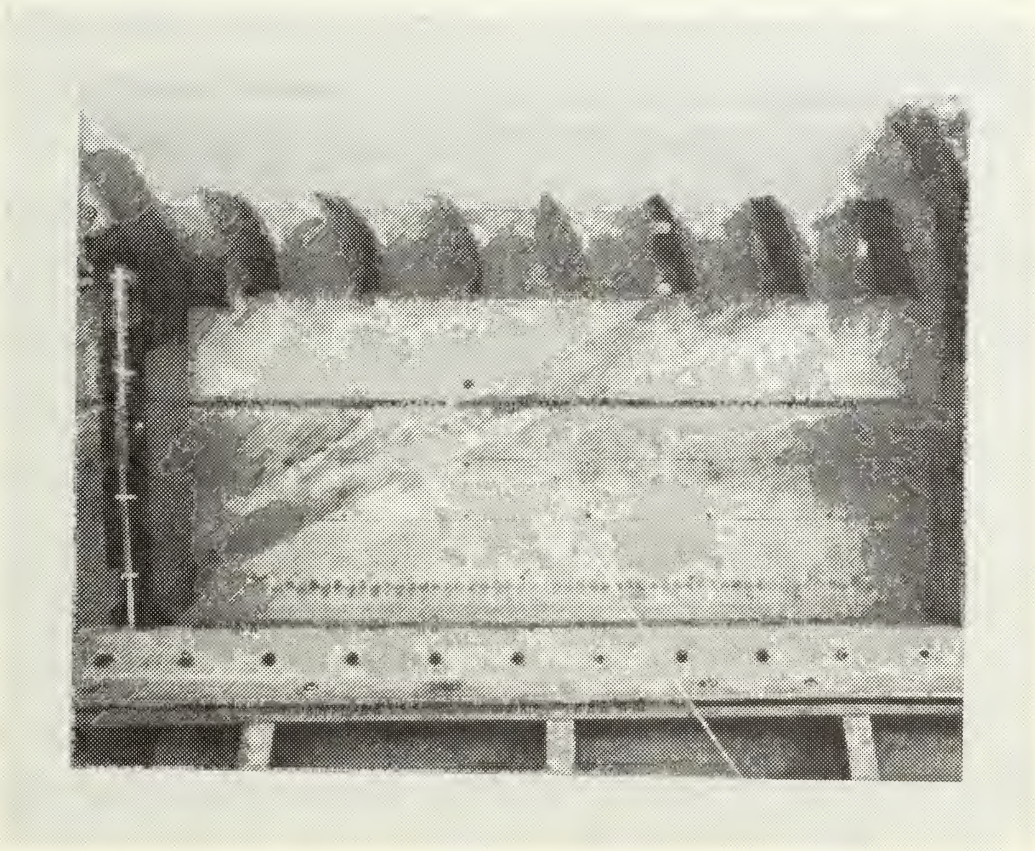

Figure 5. Cascade arrangements showing location of the sidewalls, blades, and Kiel probe below the lower measuring plane.

The inlet measurement plane was located nine inches vertically upstream of the blade leading edges. Two exit measuring planes were provided, one-half, and four inches vertically behind the blade trailing edges. The half-inch plane was found to be too close to the blades to obtain a complete indication of the wakes. The narrowness of the wakes and the steep gradients in the wakes combined with the finite size of the measuring probe made accurate mapping of the wakes impossible. All the data presented here was obtained using the measuring plane four inches (one-half chord length) downstream of the blades.

The blades used were NACA 65-(15)10 airfoil sections. The design camber angle was 37.6 degrees, with a blade height of ten inches and a chord length of eight inches. The resulting solidity was therefore equal to unity.

B. INSTRUMENTATION

Measurements at the inlet and outlet measuring planes were made with United Sensor and Control Corporation YC-120 flow probes, which are two-dimensional, directional probes. These probes had three sensing holes on a wedge-shaped prism measuring section. Two holes, one on each side of the wedge, gave an indication of the static pressure.

They also allowed the sensing of the direction of the flow by rotating the probe about its axis until the pressures at these two holes were equal. The total pressure was sensed at the center hole on the leading edge of the wedge when the

probe is directed into the flow. The dynamic pressure was determined by the difference of the total pressure and the average of the side hole pressures. This value was corrected because the side pressures are not exactly equal to the actual static pressure in the flow. The calibration and correction function of the probes were described by Woods in Ref. 6.

The probes were mounted in traversing carriages at the upper and lower measuring planes. The lower (upstream) carriage was mounted on, and extended through, the steel rear wall of the cascade test section. The upper (downstream) carriage was mounted on an adjustable frame shown in Fig. 6, and extended through a slot in the Plexiglass front wall. All measurements were made half-way between the front and rear walls, that is, at the mid-span of the blades.

The horizontal locations of the probes and the flow angles sensed by the probes were read on the Systron-Donner model 160-11 automatic data-logger system described in detail by Woods in Ref. 6. The probe locations along the cascade axis could be measured with an accuracy of about ±0.020 inches. The angles could be determined to an accuracy of ±0.5 degrees.

All pressure measurements in the cascade were taken with manometers connected as shown in Fig. 7. A ten inch Meriam micromanometer was used for reading the difference between the Kiel probe total pressure and the wedge probe total pressure with an accuracy of ±.005 inches of water. All other cascade pressure readings were

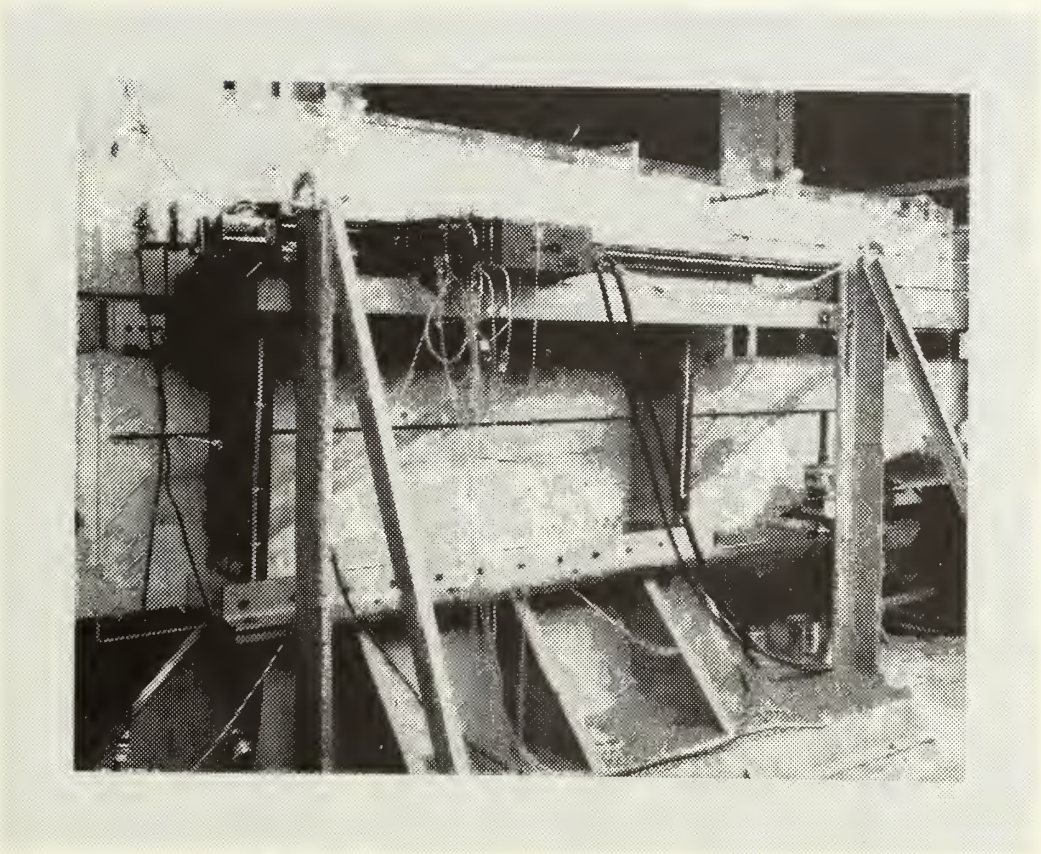

Figure 6. Cascade arrangement showing the upper traverse and support frame in place.

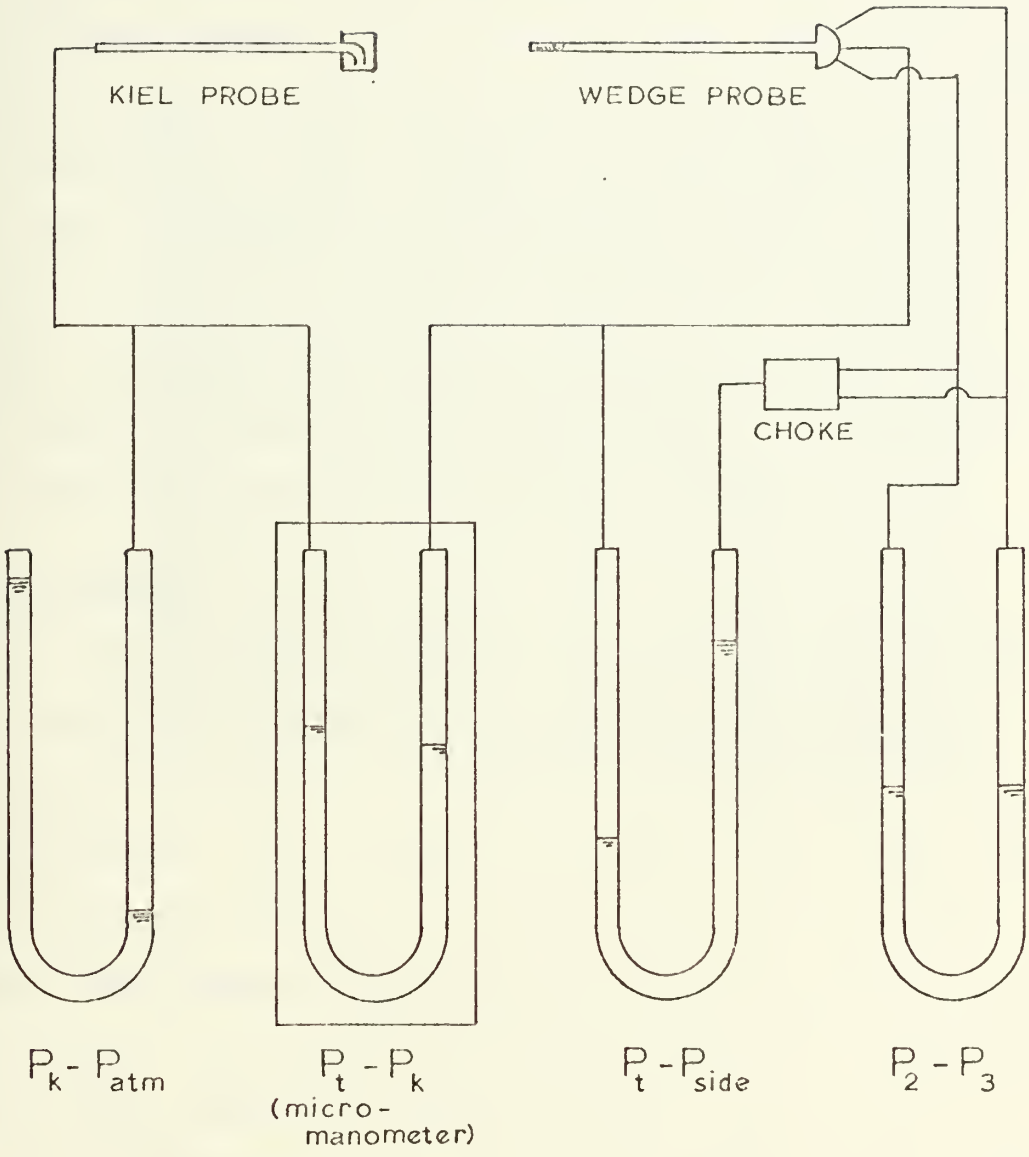

FIGURE 7. Arrangement of pressure sensors for either upper or lower cascade traverses.

determined with glass U-tube manometers with an accuracy of ±.05 inches of water. The manometers are shown in Fig. 8.

The uncertainty of the value of Y when determined by the methods of Ref. 7, using the values given above, resulted in an uncertainty of .0103. Since the uncertainty was of the same order of magnitude as the expected reading, more than one set of data was required for each test configuration.

The Kiel probe was mounted through the Plexiglass front wall upstream of the inlet measuring plane. Its location and orientation was fixed during all surveys.

C. PROCEDURES

The initial runs in the cascade were made with a blade-chord angle of -18 degrees. An inlet survey was made at intervals of 0.5 inch, for twelve inches on either side of the centerline. Four surveys were made at the outlet plane, each one over a distance of eight inches. The spacing between data points varied from 0.5 inch to 0.05 inch in the blade wakes. Two surveys were made behind the center blade and one each behind the adjacent blades. The results of these runs indicated that the values for each of the three blades were consistent with each other. Therefore the remaining runs were made in front and behind the center blade only.

The test series consisted of runs made with blade-chord angles of -18, -15, and -21 degrees with a solidity of unity.

The following values were recorded for each run: atmospheric temperature and pressure, plenum temperature, number

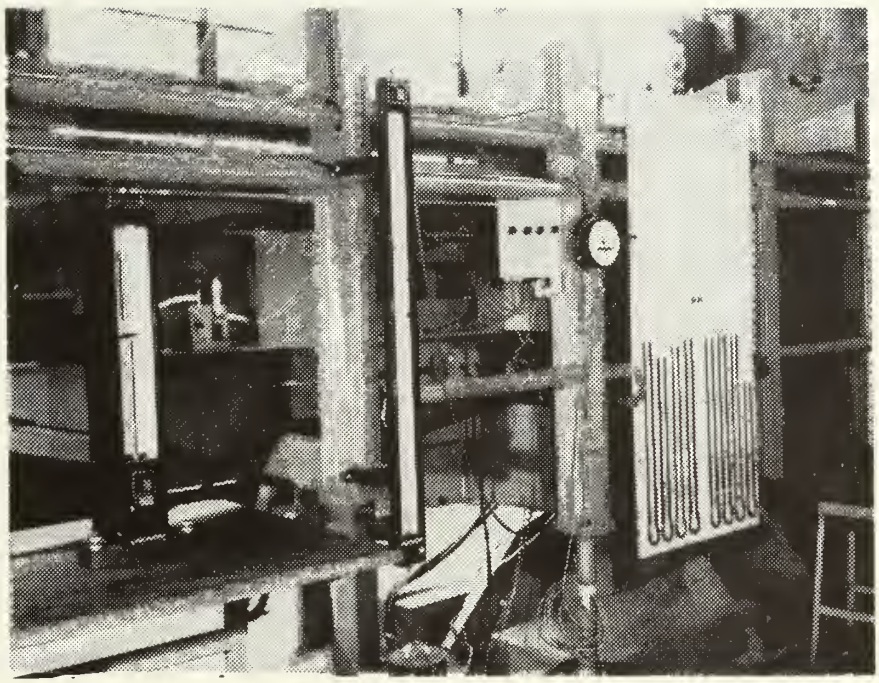

FIGURE 8. Instrumentation arrangement showing micromanometer, plenum pressure manometer, and U-tube manometers mounted on the rear wall of the cascade.

of data points before and after the blades and an average value for the Kiel probe total pressure above atmospheric pressure. At each point the traverse location, flow angle from vertical, and the following differential pressures were recorded:

$P_k - P_{atm}$

$P_t - P_k$ (Micromanometer)

$P_t - P_{side}$

The recorded pressure readings at each data point were used to calculate the two non-dimensional pressure coefficients previously described, which were read into the IBM 360/67 digital computer program of Appendix A. The computer program used the trapezoidal method of numerical integration to compute the mass averaged conditions at the inlet and exit of the test section, and the loss coefficient Y.

IV. RESULTS OF THE INVESTIGATION

A. PREDICTED VALUES

A tabulation of the predicted values of the deviation angle and loss coefficient for the range of blade-chord angles under consideration is shown in Table 1. The values are shown for all methods used to calculate each parameter.

The variation between the deduced method and Carter's rule of predicting deviation angle was about 1.5 degrees throughout the range of interest. The rate of change of deviation angle with respect to turning angle is nearly equal for both methods. This can be seen in Fig. 9, where the deviation angle is plotted as a function of turning angle.

The results of the two methods for calculating the total-pressure loss coefficient give consistent results. These results are shown in Fig. 10 where the loss coefficient is presented as a function of incidence angle.

Because in Equation 1, where corrections are made for blade thickness and thickness distribution different from the ten percent thick NACA 65 series blade, the values of $(i_o)_{10}$ and $(\delta_o)_{10}$ for deviation angle are zero, the resulting predictions are valid for other thickness of similar size with the same camber angle, such as the C-4 profiles.

TABLE 1. PREDICTED VALUES

The values tabulated are the predicted values calculated using the correlations of Ref. 1 (NASA SP-36) for the measured inlet-air angles and unit solidity for a NACA 65-(15)10 blade (camber angle 37.6 degrees).

a) Reference incidence and deviation angles.

i_0 [1]	n	i_{ref}	δ_0 [1]	m
0	-.035	-1.32	0	.17

			Deduced method			Carter's rule			
γ	β_1	i	δ_{ref}	δ	$\Delta\beta$	m_c	δ_{ref}	δ	$\Delta\beta$
-15	-.93	-4.73	6.39	6.27	26.60	2.10	7.90	7.78	25.02
-18	.18	- .62	6.39	6.41	30.57	2.09	7.86	7.88	30.34
	.31	- .49	6.39	6.42	30.69	2.09	7.86	7.89	30.20
-21	1.38	3.58	6.39	6.56	34.62	2.08	7.82	7.99	33.19
	1.54	3.74	6.39	6.57	34.74	2.08	7.82	8.00	33.34

b) Total-Pressure loss coefficient (assume $\beta_1 = 0$)

γ	i	β_2	D	θ^*/c	Y^2	Y^3
- 9	-9.8	21.80	.2715	.009	.0217	.0162
-12	-6.8	24.68	.3211	.009	.0232	.0209
-15	-3.8	27.78	.3787	.010	.0287	.0258
-18	- .8	30.41	.4311	.012	.0363	.0320
-21	2.2	33.28	.4922	.012	.0412	.0443

---

[1] assume β_1 close to zero

[2] from equation 264 Ref. 1 using $H_2 = 1.1$

[3] from Fig. 149(b) Ref. 1

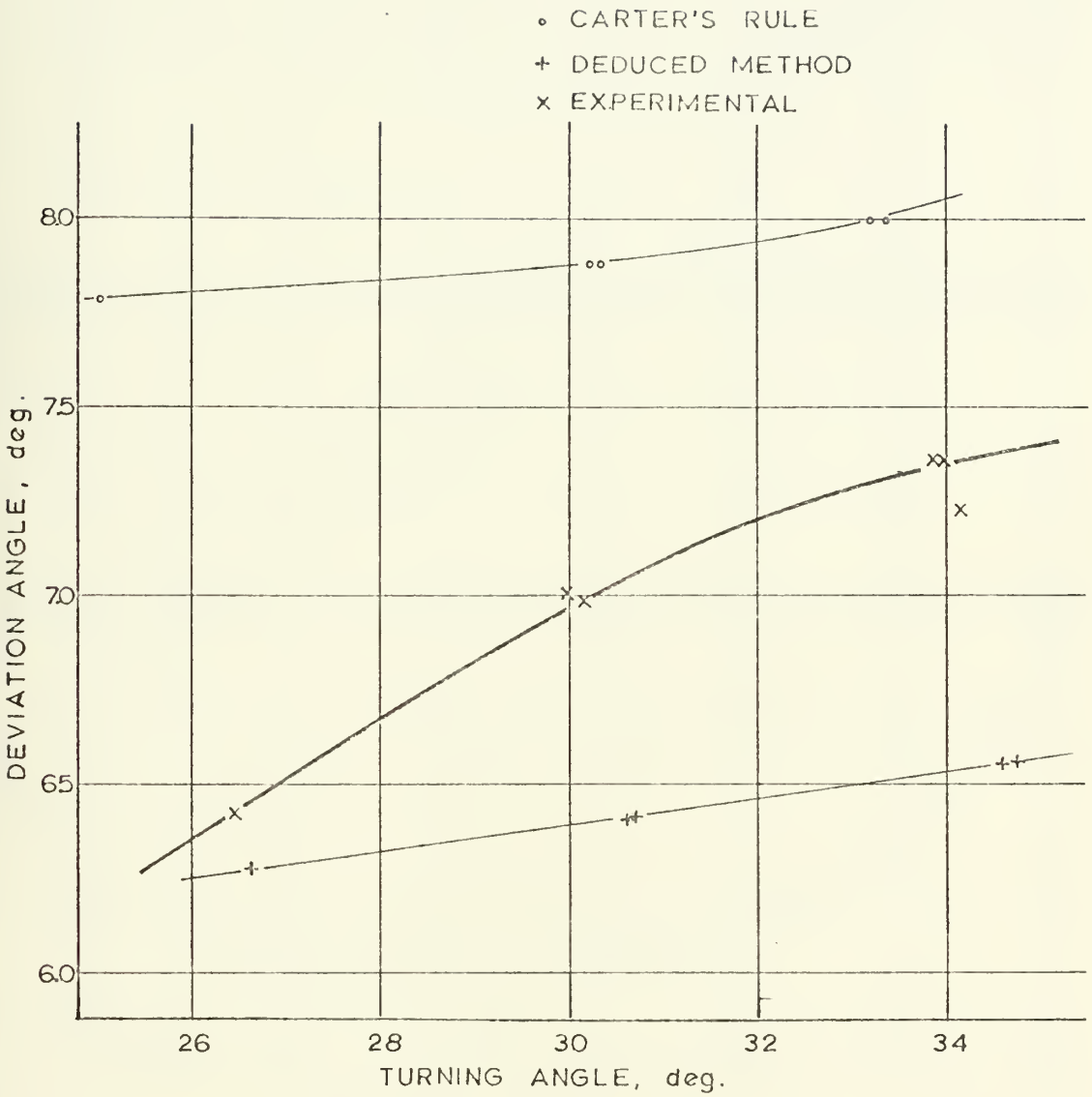

FIGURE 9. Deviation angle vs. turning angle for a NACA 65-(15)10 blade used as an inlet guide vane with unit solidity.

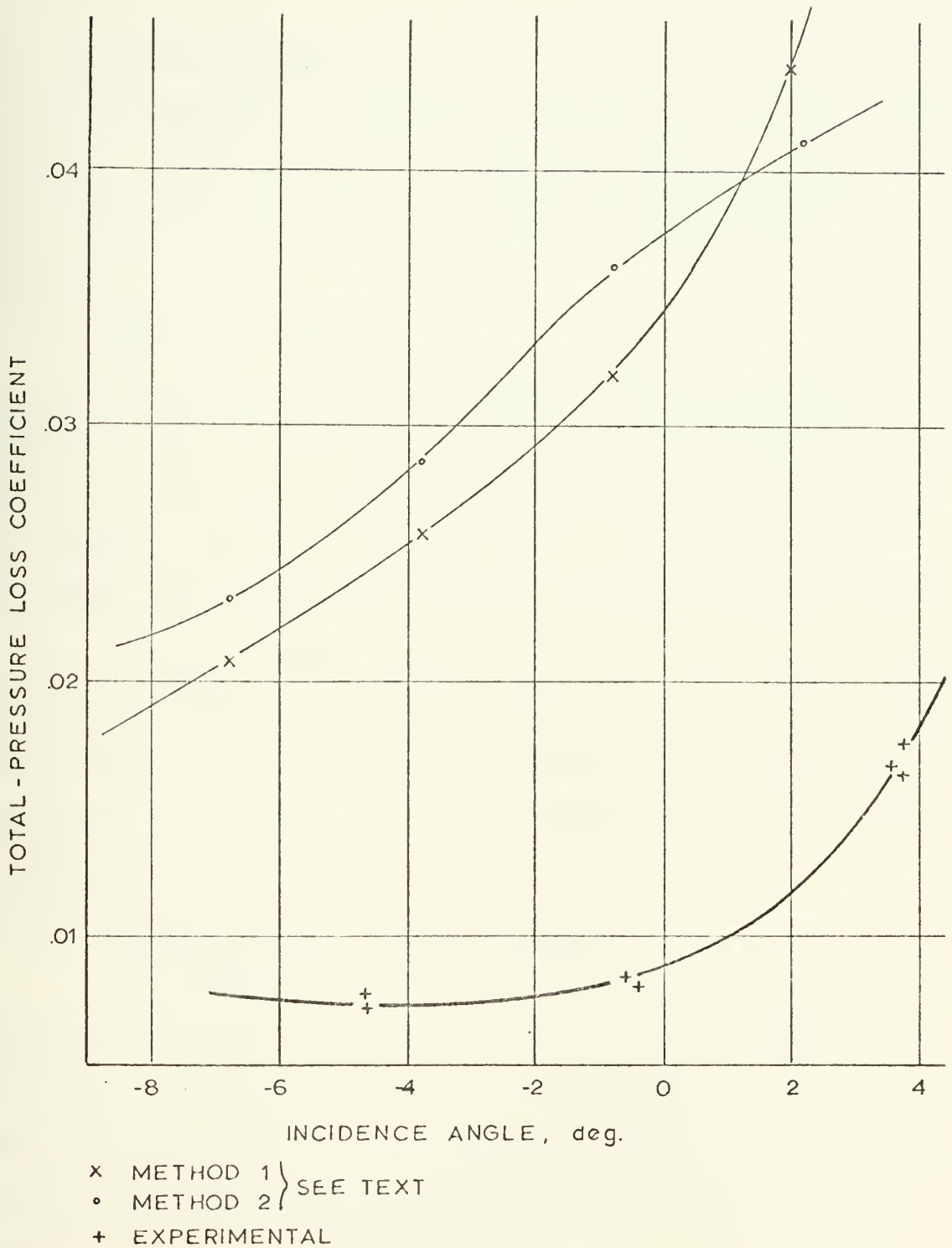

FIGURE 10. Total-pressure loss coefficient $Y = \frac{P_{t1} - P_{t2}}{Q_1}$ vs. incidence angle for NACA 65-(15)10 blade used as an inlet guide vane with unit solidity.

B. EXPERIMENTAL RESULTS

The experimental results are tabulated in Table 2. At least two runs were made at each blade-chord angle setting as a check because of the large uncertainty which was discussed earlier.

1. Deviation Angle

In Figure 9 the experimentally obtained values of deviation angle can be compared with the correlation results. The expected uncertainty of the experimental points was ±1.0 degree. However the variation of the data points was less than 0.35 degrees for any one blade-chord angle setting.

The experimental values are smaller than the values predicted by Carter's rule and larger than those obtained by the deduced method. However the slope of the curve of the experimental results in Fig. 9 was steeper than the slopes of the predicted curves.

2. Total-Pressure Loss Coefficient

The experimentally obtained total-pressure loss coefficients are plotted in Fig. 10 with the correlation results. Although the expected uncertainty was of the order of .01 for Y, the experimental results at a particular blade-chord angle setting varied less than .0015 for two runs.

A comparison of the experimental results and correlations show that neither the shape nor the values of the experimentally determined Y curve was predicted by the two correlation methods.

TABLE 2. EXPERIMENTAL RESULTS

The values tabulated are the results of experimental tests on a cascade made up of NACA 65(15)10 blades.

γ	β_1	β_2	$\Delta\beta$	i	δ	Y
-15	-.93	27.38	26.45	-4.73	6.42	.0077
						.0073
-18	.18	29.80	29.98	- .62	7.00	.0084
	.31	29.83	30.14	- .49	6.97	.0082
-21	1.38	32.44	33.82	3.58	7.36	.0169
	1.54	32.44	33.98	3.74	7.36	.0176
	1.54	32.58	34.12	3.74	7.22	.0164

V. CONCLUSIONS

From the experimental results shown in Fig. 11 the optimum setting for NACA 65-(15)10 blades used as IGV can be found. It can also be seen that there was a range of low losses from -5 to 0 degrees incidence angle in which the deviation angle varies 0.5 degrees, that is, from 6.5 to 7.0 degrees. This range would be the low-loss operating range of the blade. The predicted minimum loss incidence angle, -1.32 degrees, was in this range. The minimum loss incidence angle and deviation angle at that point were predicted by the design correlations for compressor blading with an accuracy of ±2.0 degrees. However they did not predict accurately the absolute value of the total-pressure loss coefficient or its variation with incidence angle.

Because the thickness and thickness distribution of the blade had no influence on the values of deviation angle or losses predicted, the experimental values for the NACA 65 ten percent thick blade should be applicable to any similar blade with equal equivalent camber angle including the C-4 profile about which information was desired.

Additional tests should be carried out to verify that the minimum losses were at -3 degrees incidence angle by obtaining experimental results with the same blade and solidity at blade-chord angles of -12, -9, and -6 degrees.

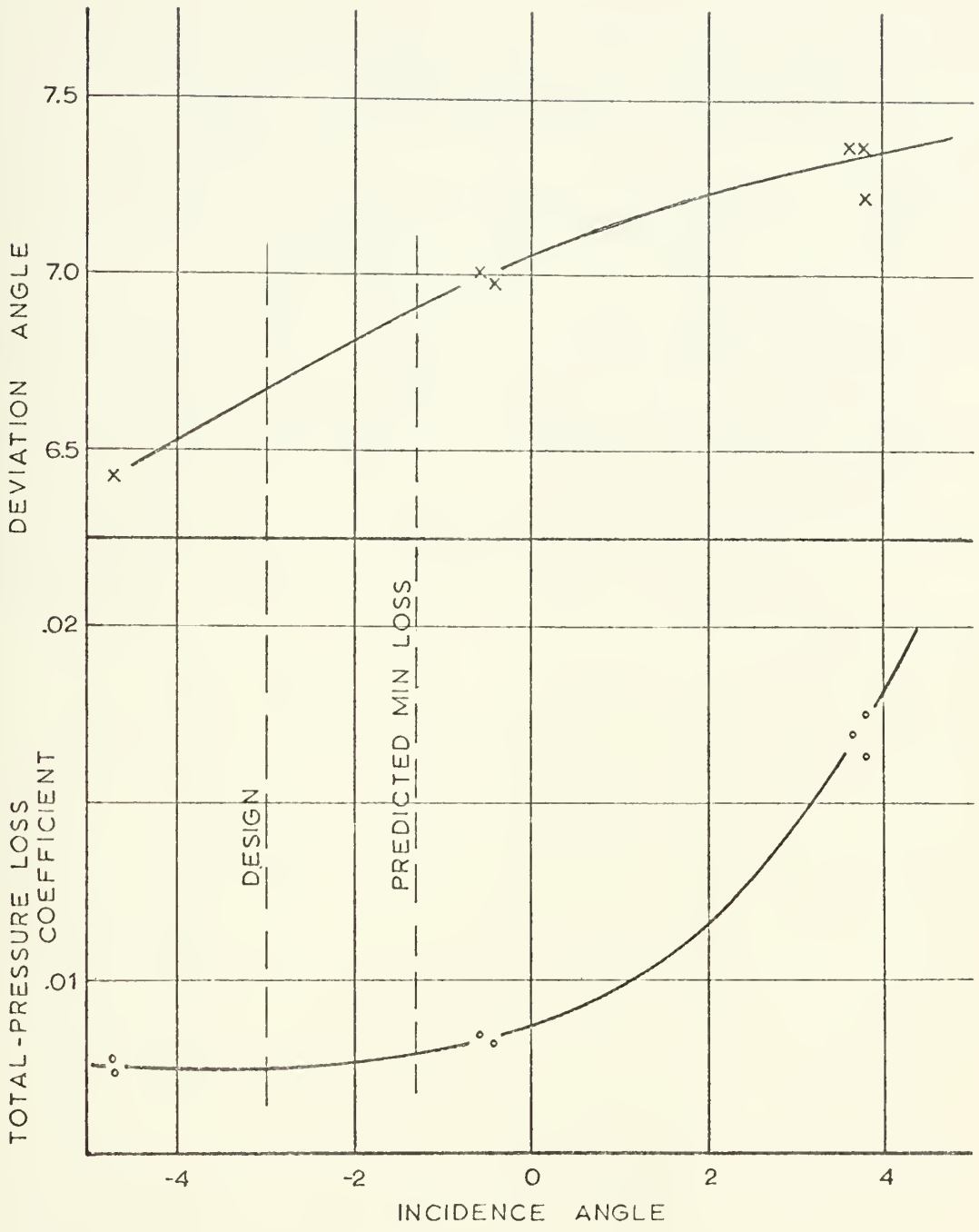

FIGURE 11. Experimental results for deviation angle and total-pressure loss coefficient vs. incidence angle for a NACA 65-(15)10 blade at unit solidity.

To find the effects of solidity the tests should also be made over the range of blade-chord angles for solidities of 0.75, 1.33, and 1.5.

However before any further testing is carried out in the Rectilinear Cascade Test Facility the first four recommendations of Ref. 3 should be considered to improve the flow conditions in the test section. The removal or redesign of the turning vanes in the plenum chamber should also be considered because during some tests wakes from the turning vanes were felt in the test section.

APPENDIX A

COMPUTER PROGRAM CASCADE III

The following program takes data of cascade tests and computes mass averaged conditions at cascade inlet and exit, and the loss coefficients Y.

The program inputs are:

INPUT	CODE	UNITS
Chord Length	C	Inches
Blade Spacing	S	Inches
Atmospheric Temperature	TATM	Degrees F
Atmospheric Pressure	PATM	Inches of Hg
Run Number	NRUN	
Number of Data Points Before Blade	NPTS1	
Number of Data Points After Blade	NPTS2	
Reference Kiel Probe Pressure	PK	Inches of Water
Plenum Temperature	TPL	Degrees F
Traverse Location	X1,X2	Inches
Total-Pressure Function	PT1,PT2	
Dynamic-Pressure Function	Q1,Q2	
Flow Angle	ALFA1,ALFA2	Degrees

```
C                    COMPUTER PROGRAM CASCADE III
CC
C   COMPUTER PROGRAM CASCADE III FOR THE REDUCTION OF CASCADE DATA FROM
C   THE INVESTIGATION OF LOSS AND TURNING ANGLE OF INLET GUIDE VANES. A
C   KEIL PROBE TOTAL PRESSURE IS USED AS A REFERENCE.
CC
C
      IMPLICIT REAL*8 (A-H,P-Z)
      DIMENSION ALFA1(99),ALFA2(99),PT1(99),Q1(99),PT2(99),Q2(99),X1(99)
     1,DX1(99),X2(99),DX2(99),V1(99),V2(99),VA1(99),VA2(99),VT2(99),RHO1
     2(99),RHO2(99),F11(99),F12(99),F13(99),F14(99),F15(99),F16(99),F21(
     399),F22(99),F23(99),F24(99),F25(99)
      REAL*8 G/32.174D0/,RG/53.3448D0/
C
C   READ CASCADE CONFIGURATION (BLADE CORD AND SPACING AND BLADE-CORD ANGLE)
C
      READ (5,80) C,S,NBCA
   80 FORMAT (2F6.3,I4)
      WRITE (6,88) C,S,NBCA
   88 FORMAT (' ',2F6.3,I4)
C
C   READ CONSTANTS AND FIXED DATA (ATOM TEMPERATURE AND PRESSURE,RUN
C   NUMBER (NRUN), NUMBER OF DATA POINTS (NPTS1,NPTS2),REFERENCE KEIL
C   PRESSURE (PK), PLENUM TEMPERATURE (TPL))
C
      READ (5,82) TATM,PATM,NRUN,NPTS1,NPTS2,PK,TPL
   82 FORMAT (F5.1,F6.2,3I4,F6.3,F5.1)
      WRITE (6,89) TATM,PATM,NRUN,NPTS1,NPTS2,PK,TPL
   89 FORMAT (' ',F5.1,F6.2,3I4,F6.3,F5.1)
C
C   READ AND PRINT INPUT DATA
C
      WRITE (6,85)
      DO 51 I=1,NPTS1
      READ (5,83) X1(I),PT1(I),Q1(I),ALFA1(I)
      WRITE (6,86) X1(I),PT1(I),Q1(I),ALFA1(I)
   51 CONTINUE
      WRITE (6,87)
      DO 52 I=1,NPTS2
      READ (5,83) X2(I),PT2(I),Q2(I),ALFA2(I)
      WRITE (6,86) X2(I),PT2(I),Q2(I),ALFA2(I)
   52 CONTINUE
   83 FORMAT (F5.2,2F5.3,F6.2)
   85 FORMAT (1H1//8X,'DATA'//4X,'X1',5X,'PT1',5X,'Q1',5X,'ALPHA1'//)
   86 FORMAT (' ',2X, F5.2,2(3X,F5.3),3X,F6.2)
   87 FORMAT (' '//4X,'X2',5X,'PT2',5X,'Q2',5X,'ALPHA2'//)
C
C   CONVERT PATM (IN.HG) TO PSIA
```

```
C
      SGHG = 13.63905D0 - (1.36303D-3*TATM)
      CFHG = (.4891585D0*SGHG)/13.54D0
      PATM = PATM * CFHG
C
C   CONVERT INPUT RATIOS TO PRESSURES
C
      DO 15 I=1,NPTS1
      PT1(I) = ((PT1(I)*PK*.03613D0)+PATM)*144.D0
      Q1(I) = Q1(I)*PK
   15 CONTINUE
      DO 16 I=1,NPTS2
      PT2(I) = ((PT2(I)*PK*.03613D0)+PATM)*144.D0
      Q2(I) = Q2(I)*PK
   16 CONTINUE
C
C   GENERATE DX1,DX2
C
      M = NPTS1-1
      DO 17 I=1,M
      DX1(I) = X1(I+1)-X1(I)
   17 CONTINUE
      L = NPTS2-1
      DO 18 I=1,L
      DX2(I) = X2(I+1)-X2(I)
   18 CONTINUE
C
C   CORRECT DYNAMIC PRESSURES FOR WEDGE PROBE ERROR
C
      DO 21 J=1,NPTS1
      Q1(J) =Q1(J)/(1.D0-.0492D0)*0.03613D0
      Q1(J) = (Q1(J)/(1.D0-.045D0))*144.D0
   21 CONTINUE
      DO 22 J=1,NPTS2
      Q2(J) = Q2(J)/(1.D0-.0492D0)*0.03613D0
      Q2(J) = (Q2(J)/(1.D0-.045D0))*144.D0
   22 CONTINUE
C
C   CALCULATE CONSTANTS
C
      GAMMA = 1.4018D0-(2.D-5*TPL)
      TPL = TPL+459.69D0
      AP2 = GAMMA*G*RG*TPL
      AA = AP2/GAMMA
C
C   CALCULATE VELOCITIES, DENSITIES, AND VELOCITY COMPONENTS ANT MEASURING
C   STATIONS AND CONVERT FLOW ANGLES TO RADIANS
C
```

```
      DO 23 J=1,NPTS1
      V1SQ =((2.D0/(GAMMA-1.D0))*AP2)*(1.D0-((1.D0-(Q1(J)/PT1(J))) **((G
     1AMMA-1.D0)/GAMMA)))
      V1(J) = DSQRT(V1SQ)
      RHO1(J) = (PT1(J)/AA)*((1.D0-(Q1(J)/PT1(J))) **(1.D0/GAMMA))
      ALFA1(J) = ALFA1(J)*1.745329D-2
      VA1(J) = V1(J)*DCOS(ALFA1(J))
   23 CONTINUE
      DO 24 J=1,NPTS2
      V2SQ = ((2.D0/(GAMMA-1.D0))*AP2)*(1.D0-((1.D0-(Q2(J)/PT2(J)))**((G
     1AMMA-1.D0)/GAMMA)))
      V2(J) = DSQRT(V2SQ)
      RHO2(J) = (PT2(J)/AA)*((1.D0-(Q2(J) /PT2(J)))**(1.D0/GAMMA))
      ALFA2(J) = ALFA2(J)*1.745329D-2
      VA2(J) = V2(J)*DCOS(ALFA2(J))
      VT2(J) = V2(J)*DSIN(ALFA2(J))
   24 CONTINUE
C
CC    COMPUTE INTEGRAL VALUES AT INLET AS FUNCTION OF X
C
      DO  53 J=1,NPTS1
      F11(J) = RHO1(J)*VA1(J)
      F12(J) = PT1(J)*F11(J)
      F13(J) = V1(J)*F11(J)
      F14(J) = (PT1(J) - Q1(J))*F11(J)
      F15(J) = ALFA1(J)*F11(J)
      F16(J) = Q1(J)*F11(J)
   53 CONTINUE
C
CC    COMPUTE INTEGRAL VALUES AT EXIT AS FUNCTION OF X
C
      DO 54 J=1,NPTS2
      F21(J) = RHO2(J)*VA2(J)
      F22(J) = PT2(J)*F21(J)
      F23(J) = V2(J)*F21(J)
      F24(J) = (PT2(J) - Q2(J))*F21(J)
      F25(J) = ALFA2(J)*F21(J)
   54 CONTINUE
C
CC    INTEGRATE IN X DIRECTION USING SUBROUTINE TRAP
C
      CALL TRAP (F11,DX1,NPTS1,F11T)
      CALL TRAP (F12,DX1,NPTS1,F12T)
      CALL TRAP (F13,DX1,NPTS1,F13T)
      CALL TRAP (F14,DX1,NPTS1,F14T)
      CALL TRAP (F15,DX1,NPTS1,F15T)
      CALL TRAP (F16,DX1,NPTS1,F16T)
      CALL TRAP (F21,DX2,NPTS2,F21T)
```

```
      CALL TRAP (F22,DX2,NPTS2,F22T)
      CALL TRAP (F23,DX2,NPTS2,F23T)
      CALL TRAP (F24,DX2,NPTS2,F24T)
      CALL TRAP (F25,DX2,NPTS2,F25T)
C
CC    COMPUTE MASS AVERAGED CONDITIONS AT INLET AND EXIT
C
      PT1M = F12T/F11T
      P1M = F14T/F11T
      V1M = F13T/F11T
      ALFA1M = (F15T/F11T)*57.29578D0
      Q1M = F16T/F11T
      PT2M = F22T/F21T
      P2M = F24T/F21T
      V2M = F23T/F21T
      ALFA2M = (F25T/F21T)*57.29578D0
C
CC    COMPUTE LOSS COEFFICIENTS
C
      EXPO = (GAMMA-1.D0)/GAMMA
      Y2 = (PT1M-PT2M)/Q1M
      ZETA2 = 1.D0 - ((1.D0-((P2M/PT2M)**EXPO))/(1.D0-((P2M/PT1M)**EXPO)
     1))
C
CC    WRITE OUTPUT HEADINGS
C
      SIGMA = C/S
      WRITE (6,81) SIGMA,NBCA
   81 FORMAT (1H1//26X,'TURBO-PROPULSION LABORATORY'/24X,'U.S. NAVAL POS
     1TGRADUATE SCHOOL'///9X,'CASCADE TESTS---SOLIDITY (C/S) =',F6.3,' *
     2 BLADE-CORD ANGLE =',I4///10X,'MASS-AVERAGED FLOW CONDITIONS AT CA
     3SCADE INLET (1) AND OUTLET (2)',6X,'LOSS'/2X,'RUN',6X,'PT1',6X,'P1
     4',7X,'V1',4X,'ALPHA1   PT2',6X,'P2',7X,'V2',4X,'ALPHA2   COEFFICIE
     5NTS'/2X,'NO.',5X,'(PSFA)  (PSFA)  (FT/SEC)  (DEG)  (PSFA)  (PSFA)
     6 (FT/SEC)  (DEG)   (Y2)  (ZETA2)')
C
CC    WRITE OUTPUT DATA
C
      WRITE (6,84)NRUN,PT1M,P1M,V1M,ALFA1M,PT2M,P2M,V2M,ALFA2M,Y2,ZETA2
   84 FORMAT (1H0,I4,F11.1,F8.1,F9.2,F8.2,2F8.1,F9.2,F8.2,2F8.4)
        STOP
      END
```

```
      SUBROUTINE TRAP (F,DX,NPTS,VAL)
C
C   SUBROUTINE TRAP COMPUTES THE  VARIOUS INTEGRALS IN THE X-DIRECTION
C   USING THE TRAPEZOIDAL RULE USING VARIABLE DX.
C
      REAL*8 F(99),VAL,DX(99)
      VAL = 0.D0
      M = NPTS-1
      DO 12 I=1,M
      SPACE = DX(I)/12.D0
      VAL = VAL + (SPACE/2.D0)*(F(I)+F(I+1))
   12 CONTINUE
      RETURN
      END
```

LIST OF REFERENCES

1. National Aeronautics and Space Administration Special Publication 36, Aerodynamic Design of Axial Flow Compressors, edited by I. A. Johnsen and R.O. Bullock, 1956.

2. Vavra, M.H., Aero-Thermodynamics and Flow in Turbomachines, p. 355, John Wiley and Sons, 1960.

3. Bartocci, J.E., An Investigation of the Flow Conditions at the Lower Measuring Plane, and in the Plenum Chamber of the Rectilinear Cascade Test Facility, Naval Postgraduate School, Department of Aeronautics Technical Note No. 66T-3, April 1966.

4. Rose, C.C., Jr., and Guttormson, D.L., Installation and Test of a Rectilinear Cascade, M.S. Thesis, Naval Postgraduate School, 1964.

5. Bartocci, J.E., Cascade Tests of the Blading of a High-Deflection, Single-Stage, Axial-Flow Impulse Turbine and Comparison of Results with Actual Performance Data, A.E. Thesis, Naval Postgraduate School, May 1966.

6. Woods, J.R., Jr., An Investigation of Secondary-Flow Phenomena and Associated Losses in a High Deflection Turbine Cascade, Ph.D. Thesis, Naval Postgraduate School, June 1972.

7. Kline, S.J. and McClintock, F.A., "Describing Uncertainties in Single-Sample Experiments," Mechanical Engineering, V. 75, pp. 3-8, January 1953.

8. Shepherd, D.G., Principles of Turbomachinery, Macmillan, 1956.

9. National Advisory Committee for Aeronautics Technical Note 3916, Systematic Two-Dimensional Cascade Tests of NACA 65-Series Compressor Blades at Low Speeds, by Herrig, L.J., Emery, J.C., and Erwin, J.R., February 1957.

10. National Advisory Committee for Aeronautics Technical Note 1954, Experimental and Theoretical Distribution of Flow Produced by Inlet Guide Vanes of an Axial-Flow Compressor, by Finger, H.B., Schum, H.J., and Buckner, H.A., Jr., October 1949.

INITIAL DISTRIBUTION LIST

		No. Copies
1.	Defense Documentation Center Cameron Station Alexandria, Virginia 22314	2
2.	Library, Code 0212 Naval Postgraduate School Monterey, California 93940	2
3.	Distinguished Professor M. H. Vavra Code 57Va Department of Aeronautics Naval Postgraduate School Monterey, California 93940	2
4.	Professor P. F. Pucci, Code 59Pc Department of Mechanical Engineering Naval Postgraduate School Monterey, California 93940	1
5.	Department of Mechanical Engineering Code 59 Naval Postgraduate School Monterey, California 93940	1
6.	LT William R. Wheeler, USN SMC 2369 Naval Postgraduate School Monterey, California 93940	1

Security Classification

DOCUMENT CONTROL DATA - R & D

(Security classification of title, body of abstract and indexing annotation must be entered when the overall report is classified)

ORIGINATING ACTIVITY *(Corporate author)*

Naval Postgraduate School
Monterey, California 93940

2a. REPORT SECURITY CLASSIFICATION

Unclassified

2b. GROUP

REPORT TITLE

Experimental Determination of Turning Angle and Losses of Axial Compressor Inlet Guide Vanes

DESCRIPTIVE NOTES *(Type of report and inclusive dates)*

Master's Thesis; December 1972

AUTHOR(S) *(First name, middle initial, last name)*

William Richard Wheeler

REPORT DATE	7a. TOTAL NO. OF PAGES	7b. NO. OF REFS
December 1972	48	10

CONTRACT OR GRANT NO.	9a. ORIGINATOR'S REPORT NUMBER(S)
PROJECT NO.	
	9b. OTHER REPORT NO(S) *(Any other numbers that may be assigned this report)*

DISTRIBUTION STATEMENT

Approved for public release; distribution unlimited.

SUPPLEMENTARY NOTES	12. SPONSORING MILITARY ACTIVITY
	Naval Postgraduate School Monterey, California 93940

ABSTRACT

This investigation experimentally determined the minimum loss incidence angle, deviation angle, and total-pressure loss coefficient for a cascade with airfoil-type blade profiles used as inlet guide vanes for an axial-flow compressor with an equivalent camber angle of 37.6 degrees and unit solidity. The experimental values were compared with values predicted using correlations based on compressor cascade tests.

DD FORM 1 NOV 65 1473 (PAGE 1)

0101-807-6811

Security Classification

A-31408

KEY WORDS	LINK A		LINK B		LINK C	
	ROLE	WT	ROLE	WT	ROLE	WT
inlet guide vanes						
axial-flow compressor						
total-pressure loss coefficient						
cascade						
deviation angle						